

Engine durability and lubricating oil tribology study of a biodiesel fuelled common rail direct injection medium-duty transportation diesel engine

Jai Gopal Gupta, Avinash Kumar Agarwal*

Engine Research Laboratory, Department of Mechanical Engineering, Indian Institute of Technology Kanpur, Kanpur, 208016, India

ARTICLE INFO

Keywords:

CRDI engine
Karanja biodiesel
Endurance test
Material compatibility
Tribological properties

ABSTRACT

Biodiesel has emerged as a viable alternative to mineral diesel in the transport sector to replace fossil fuels partially. However, long-term compatibility with engine hardware must be evaluated to ensure a smooth transition. Long-term material compatibility studies of Karanja oil methyl ester (biodiesel) blends with the hardware of a modern common rail direct injection system equipped diesel engine used in sports utility vehicles have been carried out in this investigation. A long-term endurance test was carried out in two phases, each lasting 274 h and utilizing (i) baseline mineral diesel and (ii) a 20% v/v Karanja biodiesel blended with mineral diesel (KB20). After completing the first phase, the engine was dismantled, and essential engine components were investigated for carbon deposits and physical wear using several techniques. Before proceeding with the next phase of the endurance test KB20, new engine components were installed in the engine, and then the test was executed. The KB20-fuelled engine exhibited lower wear on the valves and crankpins but higher wear of liners, piston rings, pistons, gudgeon pin, small and big end bearings of the connecting rod, and the main bearings. Fuel chemistry affected the lubricating oil efficacy and its residual useful life. Lubricating oil from the KB20-fuelled engine exhibited a higher increase in density and ash content. KB20 fuelled engine's lubricating oil underwent higher oxidation and polymerization. The surface roughness characteristics of the cylinder liner were measured before and after the endurance test for comparative wear evaluation during both phases of the endurance test. Carbon deposits on the cylinder head, piston top, and injectors were compared, and the pistons of the KB20 fuelled engine exhibited higher carbonaceous deposits. Biodiesel blends harmed the CRDI engine's fuel injection system. Biodiesel harms the fuel injection equipment (FIE) of the CRDI engine. Various tribological tests were performed on the lubricating oil samples collected regularly to examine the compatibility of KB20 vis-à-vis mineral diesel. This series of tribological tests on the lubricating oil samples assessed the effect of fuel chemistry on the lubricating oil's performance and residual useful life. Tests included variations in lubricant density, viscosity, flash point temperature, moisture content, pentane and toluene insoluble, and copper corrosion with time. The study summarily concluded that Biodiesel blends could be utilized in a CRDI engine without causing major engine durability or lubricating oil degradation issues.

1. Introduction

Fast depleting energy resources and galloping environmental pollution woes are the main issues staring at the world today. For maintaining the living standards and modern lifestyle, energy is essential. In the 21st century, the primary challenge for the researchers is to satisfy the galloping global energy demand [1]. Biofuels are being explored as alternatives to conventional fossil fuels. Biodiesel is an important renewable biofuel candidate being evaluated in several parts of the world. However, automotive manufacturers are challenged by biodiesel

properties, such as higher viscosity, inferior oxidation stability, and material compatibility issues. Since biodiesel has a chemical composition different from mineral diesel, its compatibility with modern engine components is suspect. Therefore material compatibility aspects need to be addressed before its wider use as an alternate fuel.

Gopal and Raj [2] conducted a comparative study to assess the durability of a single-cylinder compression ignition (CI) engine fuelled with a 20% Pongamia Oil Methyl Ester blend (PME20) and diesel, respectively. Various tribological properties of the lubricating oil samples drawn from the engine were used to assess the impact of fuel

* Corresponding author.

E-mail address: akag@iitk.ac.in (A.K. Agarwal).

<https://doi.org/10.1016/j.wear.2021.204104>

Received 26 April 2021; Received in revised form 6 September 2021; Accepted 10 September 2021

Available online 17 September 2021

0043-1648/© 2021 Elsevier B.V. All rights reserved.

chemistry on the lubricating oil properties and engine durability. These properties included kinematic viscosity, density, total base number, moisture content, ash content, pentane, and benzene insoluble. Due to its corrosiveness, hygroscopic nature, susceptibility to oxidation, and deposit formation tendency, PME 20 exhibited inferior lubricity during the long-term endurance test. Ferrography tests conducted on the lubricating oil samples exhibited relatively larger wear debris for the PME20 fuelled engine. Dhar and Agarwal [3] performed a 250 h endurance test on a direct injection compression ignition (DICI) engine to investigate the effect of 20% v/v Karanja biodiesel blend (KB20) on the engine wear and endurance vis-à-vis mineral diesel. According to the wear characterization study of liner surface, the surface texture of cylinder liners exhibited similar deterioration after the durability test for both fuels. On the anti-trust side of the cylinder liner, scratches were observed in addition to the honing marks in the KB20 fuelled engine, which indicated relatively higher liner wear caused by KB20. However, Dhar and Agarwal [3] reported that biodiesel-fuelled engines exhibited relatively lower wear of piston rings, pistons, and small end bearings of the connecting rods. They found higher carbon deposits on the piston top, cylinder head, and injector tip of the KB20 fuelled engine than baseline mineral diesel-fuelled engine, possibly due to higher carbon residues and lower volatility of biodiesel. Biodiesel's lower volatility increased the heat release during the late combustion phase, resulting in lesser time for the in-cylinder soot oxidation, which caused unburned/pyrolyzed biodiesel products to condense on the combustion chamber walls, resulting in increased carbon deposits [3]. Tziourtzioumis et al. [4] investigated a B70 fuelled common rail direct injection (CRDI) diesel engine under steady-state and transient conditions for 30 h. They discovered thick slurry rich in fatty esters in the fuel filters, in addition to experiencing initial engine starting issues. Injector nozzle holes were also covered by thick, oily carbonaceous deposits [4]. Fazal et al. [5] compared engine component wear from biodiesel and mineral diesel-fuelled engines. They discovered lower/comparable wear of biodiesel/biodiesel blend fuelled engine components vis-à-vis mineral diesel-fuelled engine during the field trials. Armas et al. [6] performed a 600 h accelerated endurance test to compare the effects of ethanol-biodiesel-diesel blend (7.7%–27.69% - 69.61% v/v) vis-à-vis baseline diesel in a CRDI diesel engine. According to this study, both test fuels exhibited similar effects on the fuel injection system components [6]. Carbon deposits in the combustion chambers of biodiesel and diesel-fuelled engines were reported by Pehan et al. [7]. Agarwal et al. [8] used a 512 h endurance test to investigate the effect of B20 (Linseed oil methyl ester) on the wear of CI engine components. They detected a significant reduction in carbon deposits on the piston top of the B20 fuelled engine. Because of the additional lubricity of biodiesel, the physical wear of critical engine components was ~ 30% lower in the B20 fuelled engine. Lubricating oil samples were also analyzed to validate these physical wear measurement results. The B20 fuelled engine's lubricating oil samples exhibited relatively lower ash content, indicating the presence of a lower wear debris [8]. Staat and Gateau [9] published findings of their three-year study, which used RME in 2000 vehicles in France. They reported a reduction in lubricating oil viscosity for the vehicles using more than 30% RME blends. The wear and cleanliness of RME-fuelled engines, on the other hand, was comparable to or even better than the ones using mineral diesel. Sem [10] reported deposits on the piston skirt and ring groove in the four biodiesel-fuelled engines under investigation. On the other hand, such deposits were absent in the diesel-fuelled engines investigated in this study. Fazal et al. [11] compared the corrosive properties of mineral diesel and Palm biodiesel for engines/vehicles and took weight loss and corrosion rates into consideration. Palm biodiesel was more corrosive to copper and aluminum components than mineral diesel. On the other hand, stainless steel was completely biodiesel compliant [11]. Kaul et al. [12] also compared the corrosiveness of biodiesels (*Jatropha curcas*, *Karanja*, *Mahua*, and *Salvadoran oleo ides*) to the piston, liner, and other components, compared to baseline mineral diesel. Biodiesel produced from

Salvadoran oleo ides (*Pilu*) was the most corrosive, followed by *Jatropha curcas*. *Karanja* and *Mahua* biodiesels produced corrosion comparable to baseline mineral diesel [12]. Biodiesel emerged to be largely incompatible with nitrile rubber, nylon 6/6, and high-density polypropylene in a study conducted by Besee and Fay [13]. On the other hand, Teflon and Viton were relatively more compatible with B100 [13]. During biodiesel oxidation, hydroperoxide forms, an unstable compound that attacks the elastomers, concluded Gerpen [14]. According to Schumacher et al. [15], rubber components of the fuelling device degraded upon exposure to biodiesel. However, Viton (fluorinated rubber), steel, aluminum, and nylon reinforced tubings were found to be biodiesel compatible.

Biodiesel has potential unsuitable fuel characteristics such as lower oxidation stability, higher hygroscopicity, higher electrical conductivity, polarity, and solvency, all contributing to increased corrosion of metallic components and degradation of elastomeric components [16]. The results of using rice bran oil-based biofuels on the lubricating oil degradation, deposit formation, wear of diesel engines were analyzed by Hoang et al. [17]. Owuna [18] reviewed several studies on the thermo-oxidative stability of vegetable oils to validate their utility as an alternate and sustainable energy source.

Since studies on these aspects are scarce, comprehensive research on biodiesel engine durability is needed to understand the wear mechanisms. Engine component durability depends on the lubricating oil quality and deterioration over time and usage. Lubricating oil gets contaminated because of dilution from fuel and wear debris. Lubricating oil dilution is affected by the physical properties of the fuel. Hence, the effect of biodiesel on lubricating oil degradation must be investigated. Lin et al. [19] evaluated how biodiesel (Palm biodiesel and blends; B100 and B20) affected the lubricating oil degradation in a heavy-duty diesel engine operating for 300 h (18,000 km). The viscosity decreased by 11.9 cSt, and the total alkalinity increased to 8.24 mg KOH g⁻¹ from 7.89 mg KOH g⁻¹ at the start. B100 and B20 engine's lubricating oils had total alkalinity of 8.26 and 8.05 mg KOH g⁻¹, respectively. The contribution of palm biodiesel to lubricating oil degradation was negligible though [19]. Biodiesel (B100) and baseline diesel were also tested in two identical unmodified vehicles to realistically determine various aspects of biodiesel's compliance with modern CRDI fuel injection equipment (FIE) to evaluate biodiesel's long-term durability/compatibility with engine components in a 30,000 km field trial under identical operating conditions [20,21]. Engine reliability problems, including fuel filter plugging, injector coking, piston ring sticking, carbon deposits in the combustion chamber, and leakage of lubricating oils, were relatively lower in the biodiesel-fuelled vehicle during the field trials [20]. Until biodiesel is adopted in current CRDI vehicles on a large scale, the researchers recommend that OEMs undertake further active technical measures to overcome these technical challenges [21]. In a separate analysis, Dhar and Agarwal [22] detected higher trace metals, such as Fe, Cu, and Mg, in the lubricating samples drawn after a 200 h test with B20 vis-a-vis baseline mineral diesel. Dandu and Nanthagopal [23] investigated the lubricating oil degradation in a compression ignition engine using 100% *Karanja* oil methyl ester in a long-term durability analysis. The experiments were split into two phases of 256 h each. It was reported that the trace concentrations of wear metals in the lubricating oil samples drained from the *Karanja* biodiesel (B100) engine were relatively higher than that of baseline diesel engine [23].

Staat and Gateau [9] reported that the viscosity of lubricating oil reduced slightly more in the fleet having 2000 vehicles using RME during the field trials. RME blends, on the other hand, had no discernible impact on oil change interval [9]. Thornton et al. [24] reported that Soy biodiesel (B20) fuelled engines exhibited higher lubricating oil dilution than the baseline mineral diesel-fuelled engine. Analysis of wear metal traces present in the lubricating oil provides useful information on the engine component wear. The traces of wear metals present in the lubricating oil could determine the extent of wear of the engine components. Agarwal et al. [25] detected relatively lower trace

concentrations of wear metals in the lubricating oils drawn from the B20 fuelled engine than baseline mineral diesel-fuelled engine. Trace metals in the lubricating oil samples drawn from Soyabean methyl ester (SME; B100) and baseline mineral diesel-fuelled engine were detected by Schumacher et al. [15]. B100 fuelled engine's lubricating oil exhibited a lower trace concentration of Pb, Fe, and a higher trace concentration of silicon, while comparable trace concentrations of Cu and Cr [15]. Sentanuhady et al. [26] investigated the effect of B20 and B100 during long-term operation on the trace metals and chemical compound contamination of the lubricating oil in a diesel engine. The average concentrations of Fe, Al, and Cr trace metals in B100 fuelled engine's lubricating oil were 28, 13.5, and 42% lower, and Cu and Pb trace metals were 23 and 19% higher, respectively, compared to the lubricating oil samples drawn from B20 fuelled engine [26]. In a 80,000 km field trial of two pickups, Reece and Peterson [27] identified appreciable levels of trace metals in the lubricating oil samples drawn from mineral diesel and RME (B20) fuelled vehicles. Sem [10] concluded that synthetic lubricating oils were longer lasting and more tolerant to B100 usage due to special additives used for enhancing their residual useful life (RUL), thus reducing the piston skirt deposits. Mosarof et al. [28] performed experiments with Calophyllum biodiesel blends (PB10, PB20, PB30, CIB10, CIB20, and CIB30) at different engine speeds (1000–2400 RPM) at full load. Lower wear scar surface area and superior engine performance were reported in PB20 compared to baseline mineral diesel. Murugesan et al. concluded B20 to be a more suitable alternative fuel for diesel engines in a review article [29]. Patel et al. [30] examined waste cooking oil (WCO), Jatropha, and Karanja oils in a Genset engine vis-à-vis baseline mineral diesel to study its effect on trace metal emissions. Raadnu and Meenak [31] detected identical trace levels of wear metals in the lubricating oil samples drawn from refined Palm oil and mineral diesel-fuelled vehicles. The wear of Al, Fe, Cr, and Pb-containing components in a CI engine decreased when biodiesel was blended with mineral diesel [32].

A few challenges for large-scale biodiesel adoption include lubricating oil dilution caused by biodiesel's low volatility and inferior oxidation stability [33]. There is always a risk of unburned biodiesel getting into the oil sump and oxidizing, causing deterioration and thickening of the lubricating oil, leading to sludge precipitation and significant carbon dispersion. On the other hand, lubricating oil thinning can be caused by fuel dilution or shear of viscosity modifier polymer additives. Besides that, biodiesel traces in the lubricating oil causes metals such as copper and lead to leach from the bearings. Engine operational conditions, oil grade, engine type, and service are the factors, which influence the lubricating oil deterioration. The impact of biodiesel on the life span of lubricating oil is also not known. There is a need to understand the complicated physicochemical processes between modern engine lubricating oils and biodiesel. In this experimental study, Karanja biodiesel blend was assessed for compatibility with a Euro-IV common rail direct injection medium-duty transportation diesel engine, focusing on engine wear, durability, and lubricating oil deterioration with usage.

2. Methodology

Durability (endurance) tests were performed on an SUV diesel engine (Tata; Safari DICOR 2.2 L) according to the Indian standard code (IS: 10000 Part IX, 1980) [34]. Table 1 lists the specifications of the test engine. The schematic of the experimental setup used for performing the engine experiments is shown in Fig. 1.

The long-term endurance tests were conducted in two phases; the engine was operated with mineral diesel for baseline data generation in the first phase and KB20 in the second phase. Before commencement of the endurance test, the engine was prepared and run-in as per the manufacturer's instructions. The engine was operated for a preliminary running-in period of 10 h under the prescribed speed/load conditions (Table 2) before commencing the endurance test, as prescribed by IS:

Table 1
Technical specifications of the test engine.

Make/Model	Tata/DICOR 2.2L (BS-IV/Euro-IV)
Engine Type	16 valves, water-cooled, turbocharged, inter-cooled diesel engine with EGR
No. of cylinder	4, In-line
Valve Mechanism	DOHC
Bore/Stroke	85 mm/96 mm
Cubic Capacity	2179 cc
Max. Power Output	103 kW @ 4000 rpm
Maximum Torque	320 Nm @ 1700–2700 rpm
Compression ratio	17.5
Firing order	1-3-4-2
FIE System	CRDI
Maximum FIP	1600 bar
Fuel filter	Single-stage
Timing and Governing	ECU controlled

10000 part-V [35].

During the preliminary running-in, attention was paid to the engine vibrations and quietness. After this, lubricating oil was drained off, and the engine sump was refilled with fresh lubricating oil as specified by the manufacturer. Then the engine underwent the first phase of the long-term endurance test. After that, the engine was disassembled completely and then reassembled using new components for the second phase of the endurance test using B20 under different engine speed/load conditions. Its pistons, rings, connecting-rod bearings, crankshaft bearings, and other important components were replaced with new components. After that, the second phase endurance test was executed using a KB20.

As discussed earlier, the engine underwent preliminary running-in again before the second phase of the long-term endurance test using KB20 was executed.

The long-term endurance tests were conducted in an 8 h cycle, 34 cycles in each phase, hence 274 h in each phase. Each running cycle consisted of four 2-h repeating cycles (Table 3). Before executing the next cycle, it was ensured that the lubricating oil temperature was within ± 5 K of the room temperature. Wear was determined in both the phases by measuring the dimensions of various engine components such as the cylinder liner, piston, gudgeon pin, piston rings, connecting rod, bearing bore, and so on before and after the endurance test (as per IS: 10000 Part-V) [35]. Carbon deposits on each cylinder head, piston, and injector were photographed in both phases. Lubricating oil samples (100 ml) were collected in plastic torsion bottles from the engine sump every 20 h for performing various oil tests and the samples were kept in standardised storage conditions, free of chemical and moisture, contaminations, and out of direct sunlight exposure at 25 °C [36]. The samples were then analyzed for various parameters, including traces of wear metals. A flowchart of major tasks undertaken during the endurance test is shown in Fig. 2.

For both phases of the experiment, piston rings were weighed before and after the endurance test to measure the piston-ring wear (based on the weight loss of the rings). Major reasons for the cylinder liner wear included piston side thrust, combustion gas pressure on the piston rings, high combustion temperatures, abrasive action of dust and soot particles, and breakdown of lubricating oil film on the liner surface. For estimating the wear of cylinder liner, bore diameter was measured precisely at five different locations using bore gauges. A stylus-based surface roughness profilometer (Mitutoyo; SJ-301) was used to measure the cylinder liner's surface roughness profiles at various locations. The profilometer measured a host of parameters, namely average surface roughness (R_a), root mean square roughness (R_q), highest peak roughness (R_p), depth of deepest valley (R_v), the maximum height of the profile (R_y and R_z), the total height of the profile (R_t), etc. Surface profiles were measured at three liner locations: close to TDC (location of compression ring motion reversal), mid-stroke, and close to bottom dead

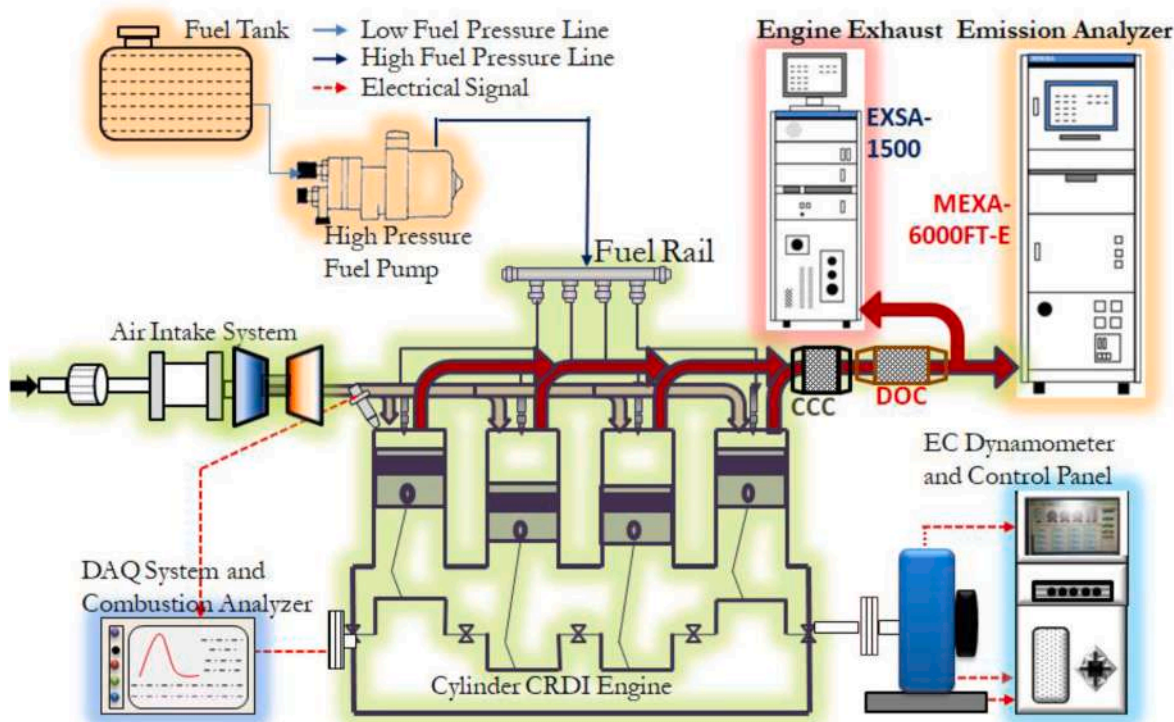


Fig. 1. Schematic of the experimental setup.

Table 2
Loading cycle for the preliminary running-in.

Engine speed (% of maximum speed)	Load (Percent of rated load)	Running Time (minutes)
Idling	0	30
40	30	30
50	30	30
70	40	30
85	40	30
40	50	30
45	60	30
50	60	30
60	60	30
70	60	30
80	60	30
75	60	30
95	60	30
100	80	30
60	80	30
70	80	30
100	100	30
70	100	30
85	100	30
100	100	30

Table 3
Engine loading cycle for the long-term endurance test [34].

Engine Speed	Load (% rated load)	Running time (minutes)
Maximum speed	75	50
Maximum torque speed	100	45
Idling	No-load	5
Maximum speed	100	20

center (BDC). These are the most critical locations in the cylinder liner from the wear viewpoint. The surface profiles were taken on both thrust and anti-thrust sides at all these three locations.

Lubricating oil analysis is the best way to analyze engine wear without disassembling the engine. Lubricating oils are a complex blend of a host of additives in a basestock, specifically designed for a particular application. Therefore characterization of the lubricating oil samples was done for both phases. Variations in the lubricating oil characteristics is primarily because of oil degradation or aging, prolonged mechanical, thermal, and environmental stresses, and foreign particle contamination from the dust and engine wear. Therefore, lubricating oil samples were analyzed for variations in their density, viscosity, ash content, flash point temperature, copper corrosion, oxidation stability, total base number, moisture content, pentane and benzene insoluble, trace metal analysis, etc. with usage in both the phases. Comparative data of the two phases was used to determine the effect of biodiesel on the CRDI SUV engine wear, deposits, and durability vis-à-vis baseline mineral diesel-fuelled CRDI SUV engine.

3. Results and discussion

Karanja biodiesel and mineral diesel’s fuel properties were determined experimentally and compared with the Indian and ASTM Specifications for biodiesel (Table 4) [29,37–41].

The results of this study are discussed in the four sub-sections. (i) Carbon deposits on the vital engine components (ii) Physical wear of the moving components, (iii) Lubricating oil tribology, and (iv) material compatibility of biodiesel vis-à-vis baseline mineral diesel.

3.1. Carbon deposits

IC engines have several in-cylinder components exposed to high temperatures and mechanical stresses during the long-term endurance test [42]. Soot deposition on these components happens due to thermal and oxidative degradation of lubricants and pyrolysis/incomplete fuel combustion. Fig. 3 shows the carbon deposits on the piston crown of mineral diesel and KB20 fuelled engines after the conclusion of the endurance test spanning 274 h.

Fig. 4 shows that the carbon deposits on the piston crowns of the

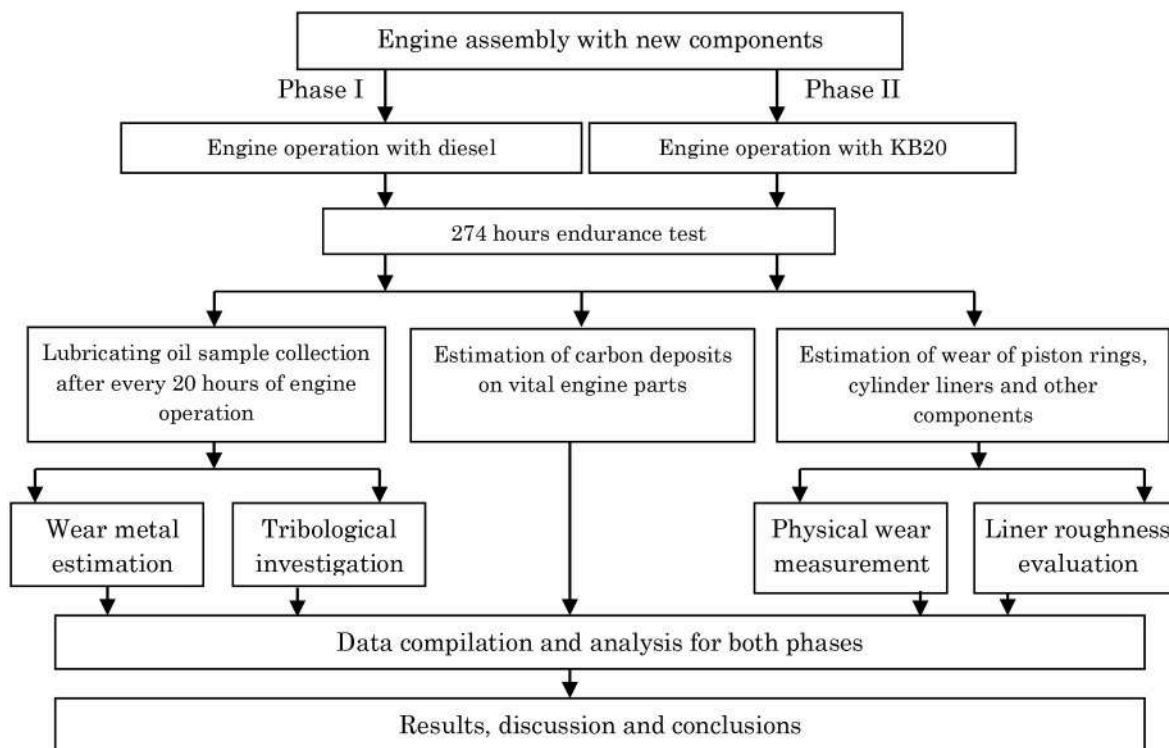


Fig. 2. Flow chart of the endurance test.

Table 4
Important test fuel properties and biodiesel specifications.

Property	IS 15607(2005) Biodiesel Specifications	ASTM 6571 Biodiesel Specifications	Karanja Biodiesel	Mineral Diesel	KB20
Density (g/cm ³) @ 30 °C	0.86–0.90	0.8–0.9	0.887	0.822	0.835
Kinematic viscosity (cSt) @ 40 °C	2.5–6.0	1.9–6.0	5.79	2.71	3.31
Flash point temperature (°C) (min.)	120	130	168	49.5	–
Ash content (%) (max.)	–	0.02	0.008	<0.005	–
Moisture content (ppm) (max.)	500	500	<200	<200	<200
Calorific value (MJ/kg)	–	–	40.36	43.06	42.52
Copper corrosiveness	Class 1	3a	1a	1a	1a
Oxidation stability (h)	6.0	–	5.25	0.97	2.27

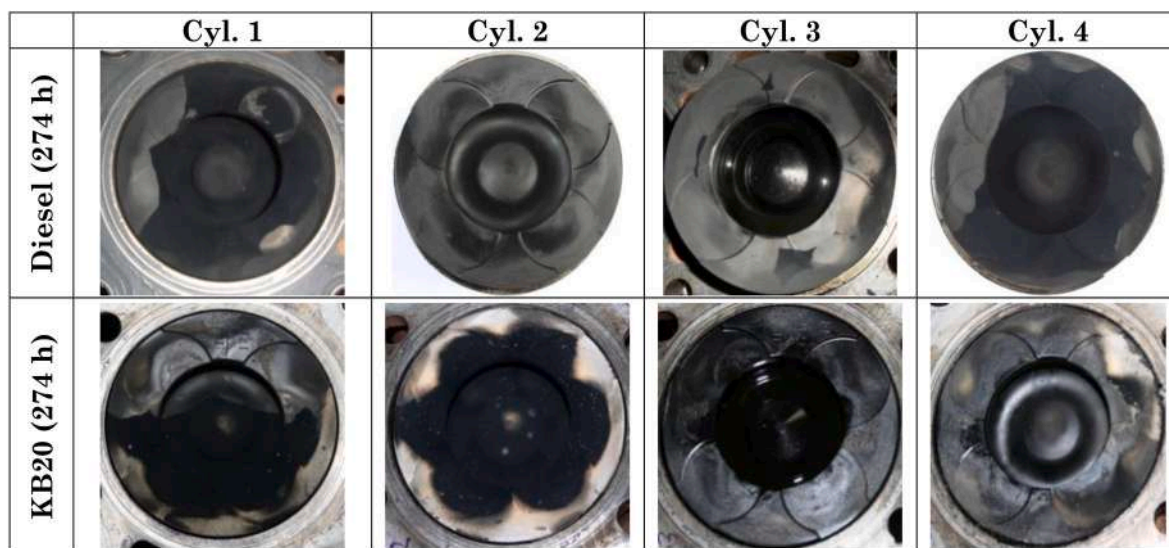


Fig. 3. Carbon deposits on the piston crowns of mineral diesel and KB20 fuelled engines.

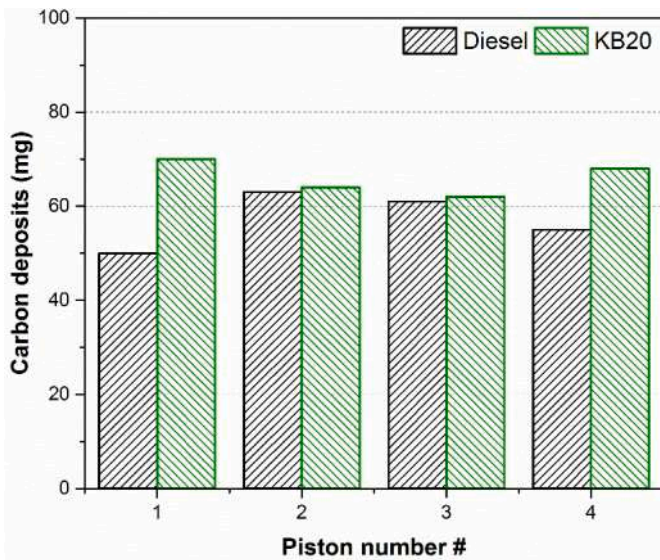


Fig. 4. Carbon deposits on the pistons of KB20 and diesel-fuelled engines.

KB20 fuelled engine were thicker. White marks on these pistons indicate higher localized thermal stresses experienced by the pistons of the KB20 fuelled engine. Quantification of carbon deposits was done by carefully removing and weighing these deposits from the piston crown, as shown in Fig. 4.

A higher mass of carbonaceous deposits was found on the pistons of the engine fuelled with KB20. This is possibly due to higher carbon residues and lower volatility of biodiesel. Since biodiesel has lower volatility, it releases more heat during the late combustion phase, leaving lesser time for the in-cylinder soot oxidation. This causes unburned/pyrolyzed sooty compounds to condense on the combustion chamber walls, increasing the carbon deposits. Agarwal and Dhar [42] also reported higher carbon deposit accumulation on the piston crowns of the biodiesel-fuelled engine. Fig. 5 shows the carbon deposits on the cylinder head in phase 1 (mineral diesel) and phase 2 (KB20) studies.

Layers of carbon deposits on the cylinder head (Fig. 5) for mineral diesel were relatively thinner, which is in line with the observations of piston crown deposits (Fig. 4). Large white marks are visible on the exhaust valves of the engine. These marks are due to higher thermal

stresses experienced by these valves, indicating higher localized temperatures with biodiesel operation. Fig. 6 shows the images for the injector deposits. Two sets of injectors were used for KB20 fuelled engine operation for 274 h. The first set of injectors was changed after 132 h of engine operation due to significant black smoke from the engine. The second set of injectors completed the remaining endurance test of the engine.

Comparatively higher carbon deposits were observed on the injectors of the KB20 fuelled engine than the baseline mineral diesel-fuelled engine. This observation was consistent for all four injectors (Fig. 6). Higher carbon residues and lower volatility of Karanja biodiesel were the reasons for higher carbonaceous deposits on KB20 fuelled engine components [43].

In a similar study, Fraer et al. [44] reported heavy sludge in B20 fuelled engines (8 nos) after 600,000 miles of vehicle operation. The existence of zinc traces in fuel, injector hole design, and residual fuel traces in the nozzle hole at the end of injection may be the factors responsible for accelerated injector deposits, according to Birgel et al. [45]. On the other hand, some other studies showed that biodiesel and biodiesel blend fuelled engines might have lower/similar carbon deposits [7,8,13,46]. Sinha and Agarwal [47] also reported that a medium-duty DIC1 transportation engine using B20 exhibited lower carbon deposits on the in-cylinder components (rice-bran oil methyl ester blend) of a direct injection transportation engine using mechanical fuel injection equipment (FIE). Mechanical and thermal stresses, carbon deposits, and chemical reactivity of test fuel were the primary causes of FIE component wear [48].

3.2. Engine wear

The wear of moving surfaces of engine components in physical contact was caused by relative motion. Mineral diesel was used as a test fuel to generate baseline wear data for assessing the impact of KB20 on engine wear during the endurance test. Then the engine was operated using KB20 under identical load/speed conditions so that the impact of biodiesel blend on the engine component wear could be compared with baseline mineral diesel. The wear was assessed by taking (i) precise measurements of physical dimensions of different critical in-cylinder moving components and (ii) the surface profiles of cylinder liners before and after each phase of the durability test using mineral diesel and KB20.

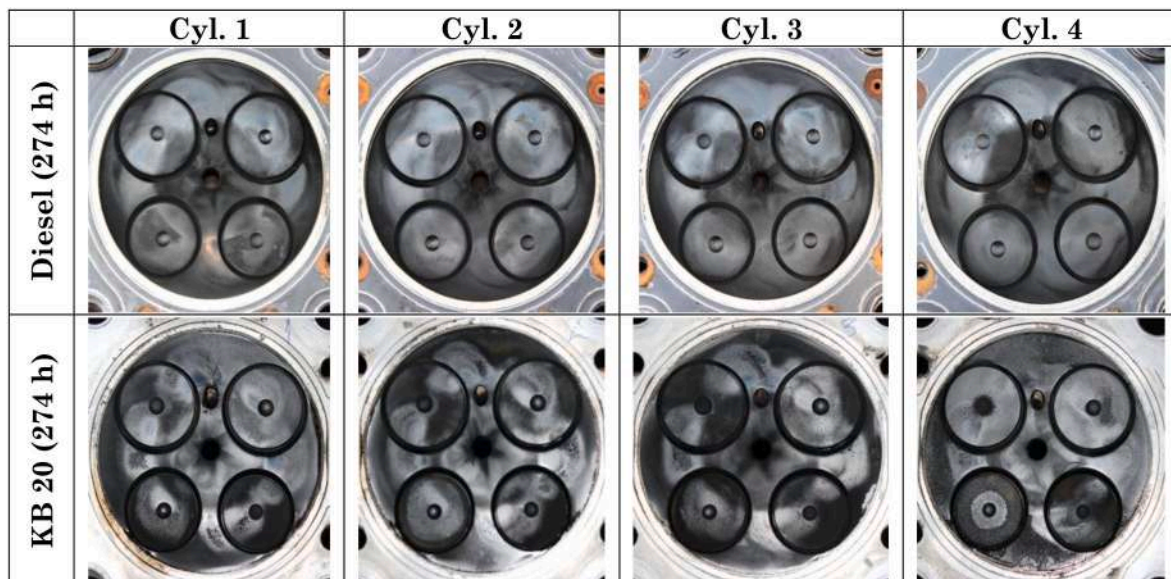


Fig. 5. Carbon deposits on the cylinder head of KB20 and diesel-fuelled engines.



Fig. 6. Carbon deposits on the injectors of KB20 and diesel-fuelled engines.

3.2.1. Physical wear

Physical dimensions of these components were measured precisely according to IS: 10000 Part V, 1980 [35]. The observations about relative wear patterns for engine operation with the two test fuels are summarized in Table 5.

For both phases of the endurance test, the wear of inlet and exhaust valve seats was measured by measuring their distance from the valve flange face using a precision dial gauge before and after the endurance test. Inlet and exhaust valves wear reduced by 52.5 and 33.1% respectively for KB20 fuelled engine, compared to baseline mineral diesel-fuelled engine. This was due to superior lubricating properties of biodiesel. Lower wear of inlet valves was observed for the KB20 fuelled engine. Lower exhaust gas temperatures at higher speeds and loads in the KB20 fuelled engine exhibited lower wear of exhaust valves than the baseline mineral diesel-fuelled engine. Fazal et al. [5] also reported a similar trend of lower wear of biodiesel fuelled engine components than the baseline mineral diesel-fuelled engine. When comparing vital moving parts such as the piston, rings, gudgeon pin, liner bore, connecting rod's small end and big end bearings, and the main bearings of the KB20 fuelled engine vis-à-vis baseline mineral diesel-fuelled engine, the wear was found to be relatively higher for the KB20 fuelled engine. The dilution of lubricating oil by fuel may have resulted in increased wear of these components. This points towards the likelihood of KB20 harming

the lubricating oil, consistent with the tribological characterization of used lubricating oil samples drawn from the oil sump periodically.

3.2.2. Piston ring weight loss

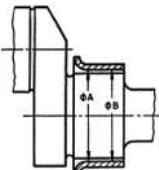
The weight loss of the piston rings after the conclusion of both phases of the endurance test was used to assess relative piston-ring wear (Fig. 7) and the effect of biodiesel on relative piston ring wear.

The KB20-fuelled engine piston rings lost more weight than the ones from the baseline diesel-fuelled engine consistently. The highest weight loss was observed for the second compression rings, and the lowest was observed for the oil rings. A possible explanation for this could be relatively inferior combustion, higher peak in-cylinder temperature, and higher soot formation in biodiesel-fuelled CRDI engines. If glycerol traces were present in biodiesel, it could lead to fuel separation, fuel filter plugging, material compatibility issues, engine deposits, and engine durability issues [49]. Kaul et al. [12] reported that Salvadoran oleo ides (Pilu) and *Jatropha curcas* origin biodiesels were more corrosive to the piston rings and liner. However, some researchers reported lower wear in biodiesel-fuelled engines in the literature review than baseline mineral diesel-fuelled engines [3,8]. However, these were DIC engines and not the CRDI engines.

Table 5
Comparison of physical wear of vital engine components of KB20 and diesel-fuelled engines.

Dimension of the component	Percentage difference in the wear of each component from KB20 fuelled engine w.r.t. baseline mineral diesel-fuelled engine (D: Lower; IN: Higher)
Distance of inlet valve head from the mounting flange face	52.52 (D)
Distance of exhaust valve head from the mounting flange face	33.13 (D)
Liner bore	50.75 (IN)
Piston diameter	177.5 (IN)
Piston rings	211.88 (IN)
Gudgeon pin, pin bore, small end bush of connecting rod	22.76 (IN)
Crankpin	12.21 (D)
Connecting rod bearing bore diameter	146.88 (IN)
Main bearing bore diameter	45.45 (IN)

Table 5 (continued)

Dimension of the component	Percentage difference in the wear of each component from KB20 fuelled engine w.r.t. baseline mineral diesel-fuelled engine (D: Lower; IN: Higher)
	

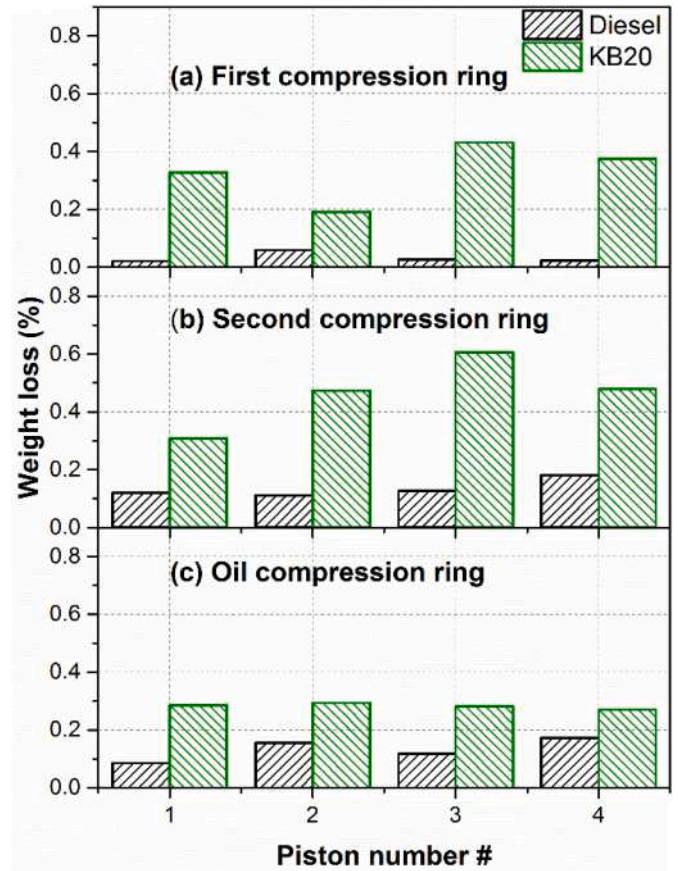


Fig. 7. Comparison of piston rings weight loss from KB20 and diesel-fuelled engines due to wear for the (a) First compression ring, (b) Second compression ring, and (c) Oil ring.

3.2.3. Liner wear

Scanning of the liner for surface roughness profiles was done for all cylinders on the thrust and anti-thrust sides to assess qualitative comparison of liner wear. The scanning positions were close to TDC, Mid-stroke, and BDC positions, as shown in Fig. 8. In both the phases, surface profiles were evaluated before and after the endurance test at the same locations. Since the test engine has a liner integral with the cylinder block and cannot be removed; hence both the tests were performed on the same liner. The piston skirt makes contact with the liner surface on the thrust side during the intake stroke and the anti-thrust side during the remaining three strokes.

R_a value denotes the arithmetic average of the roughness profile, while R_q value denotes the root mean square average over the entire evaluation length of the roughness profile. For mineral diesel and biodiesel, R_a and R_q values are shown in Table 6, and the corresponding bearing area curves are shown in Table 7 for liner 1. The deviations in

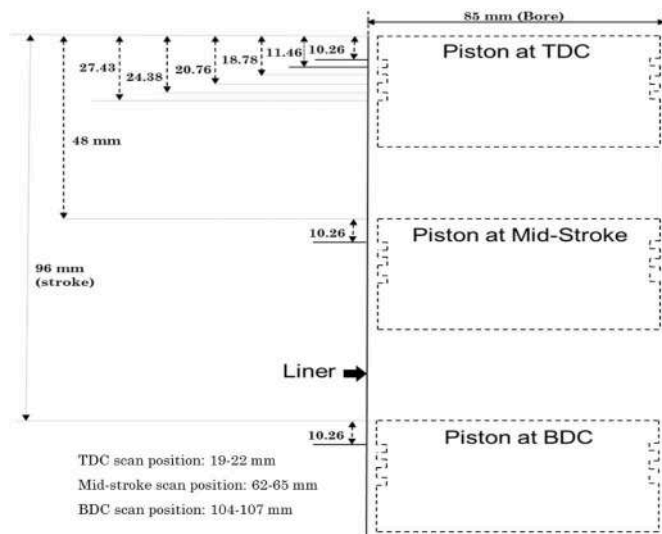


Fig. 8. Surface roughness scanning positions close to TDC, Mid-stroke, and BDC.

the surface roughness profiles before and after the durability test were used to estimate the wear qualitatively.

The anti-thrust side of the liner experienced higher wear during three of the four strokes of an engine cycle, including the power and the compression strokes, which have greater pressure and temperature. Therefore higher wear was likely on the anti-thrust side of the liner. Higher wear of cylinder liner on the antithrust side than the thrust side was also reported by other researchers [3,47,50]. These patterns were correlated to the piston motion and piston tilt as the piston traverses during various strokes. It was reported that during the four strokes of the piston, the main contact is on the antithrust side during the compression, expansion, and exhaust strokes. Contact occurs on the thrust side during the intake stroke only, when cylinder pressure and temperature are comparatively lower [3,47,50], leading to relatively lower wear. At all locations, mineral diesel and KB20 fuelled engine liners experienced equal wear. The bearing area curve (BAC) is a useful parameter for describing how the surface profile of the liner wears out over time. When slicing the material at a certain height, bearing area curves reflect the profile's material ratio as a function of the slice thickness [51,52]. The bearing area curve becomes flatter after significant wear of the liner surface, indicating removal of surface roughness peaks, e.g., in a honed surface. The shapes of the BACs show that KB20 and mineral diesel-fuelled liners wear similarly, and there was hardly any noticeable difference in the liner wear patterns of the two phases.

3.3. Lubricating oil tribology

Various analyses of lubricating oil samples were performed to determine the effect of KB20 and baseline mineral diesel on the lubricating oil deterioration in an unmodified CRDI SUV engine. This is an indirect method of wear assessment of the engine components and is limited to only broad finger-pointing. Fig. 9 depicts the density and viscosity differences of lubricating oil samples drawn from the oil sumps of mineral diesel and KB20 fuelled engines at 20 h intervals.

3.3.1. Density

The lubricating oil's density is impacted by the addition of wear particles, ambient dust, dilution by fuel, and humidity addition during the engine operation. The density of oil samples from both engines increased with usage (Fig. 9). The engine's first 20-h operation showed a faster increase in the density of the lubricating oil. The density increased faster in the KB20 engine than the baseline diesel-fuelling engine (Fig. 9). The fuel dilution decreased the density of the lubricating oil

since the density of test fuels was lower than fresh lubricating oil. The test fuel's viscosity, density, and surface tension influence the spray droplet size distribution. Larger spray droplets of KB20 resulted in higher fuel dilution of the lubricating oil with usage [49,53]. Lubricating oil polymerized due to thermal stresses encountered in presence of moisture, increasing its density with usage. Wear debris addition, ambient dust accumulation, lubricating oil polymerization, and moisture addition increase the density of the lubricating oil, whereas the fuel dilution reduces it. As a result, trends in density variations alone provide only very broad insights into wear but no definitive information of the comparative impact of KB20 on the health of lubricating oil with usage vis-à-vis baseline mineral diesel.

3.3.2. Viscosity

The lubricating oil film thickness is affected by insufficient viscosity, resulting in excessive wear of mating parts and bearings [54]. Fig. 9(b and c) shows lubricating oil samples' viscosity from KB20 and baseline mineral diesel-fuelled engines measured at 40 °C and 100 °C, respectively. After filtering the lubricating oil samples through a 75- μ m filter to remove suspended impurities and wear debris, kinematic viscosities at two temperatures were determined. The viscosity of lubricating oil samples increased with usage for both test fuels. During the entire test period, relative viscosity increase was lower in the lubricating oil samples drawn from mineral diesel-fuelled engines than the KB20-fuelled engines, as shown in Fig. 9(b and c). The viscosity of lubricating oil increases due to oxidation or polymerization while it decreases because of fuel dilution. The pattern of viscosity variation with usage suggests a higher degree of polymerization and wear debris addition of KB20 fuelled engine's lubricating oil, causing a faster rate of viscosity increase due to "fuel induced oxidation" of the lubricating oil base-stock. An engine operating with more viscous lubricant requires higher energy to produce the same brake power because of increased interfacial friction in the engine's mating surfaces. This extra energy is used to overcome the viscous drag, increasing BSFC and reducing BTE for KB20 fuelled engine than the baseline mineral diesel-fuelled engine [55,56].

3.3.3. Ash content

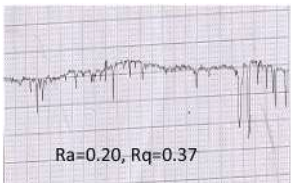
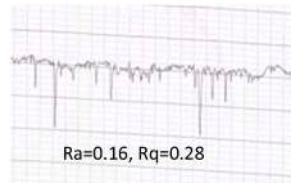
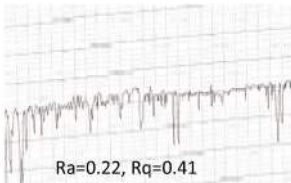
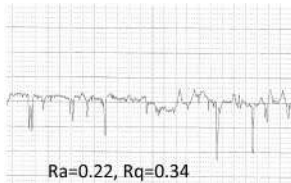
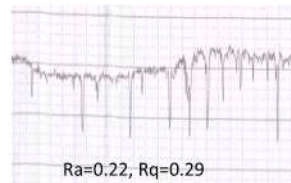
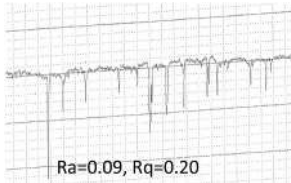
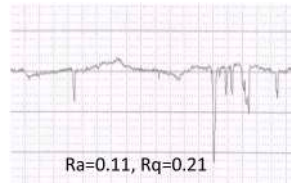
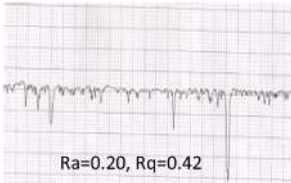
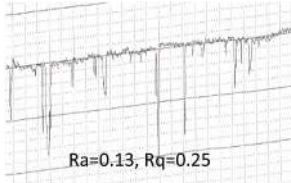
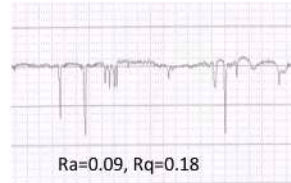
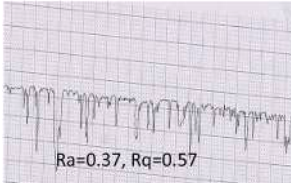
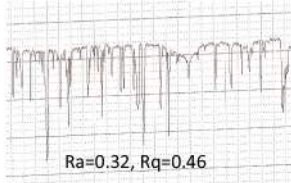
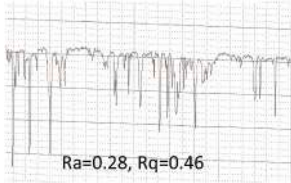
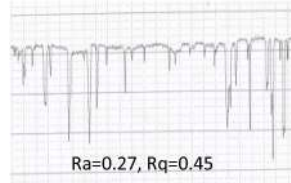
Carbonaceous materials such as lubricating oil, soot, gasoline, and non-metallic portions of the organo-metallic additives eventually become CO₂ after thermal decomposition; therefore, the ash content in the lubricating oil samples represents only the non-carbonaceous materials present in the lubricating oil. The differences in the ash content of the lubricating oil samples drawn from the mineral diesel and KB20 fuelled engines are shown in Fig. 10.

Changes in the ash content of the lubricating oils with use suggest addition of metallic wear debris and foreign particles such as ambient dust. The slightly higher ash content of the lubricating oil samples drawn from the KB20-fuelled engine than the mineral diesel-fuelled engine indicates a relatively higher metallic wear-debris in the KB20 fuelled engine. This conclusion, however, must be verified by using inductively coupled plasma-optical emission spectroscopy (ICP-OES) to quantify trace concentrations of wear metals present in the lubricating oil samples, which is discussed in a subsequent section.

3.3.4. Total base number

The Total Base Number (TBN) measures the lubricating oil's reserve alkalinity, which indicates its capacity to withstand the impact of corrosive acids produced during the engine usage. A positive TBN value indicates the absence of strong free acids in the lubricating oil. Fig. 10 shows the changes in TBN of the lubricating oil samples drawn from mineral diesel and KB20-fuelled engines with usage. TBN decreased with usage for the lubricating oils collected from both mineral diesel and KB20 fuelled engines. However, TBN reduction in the lubricating oil samples drawn from the KB20 engine with usage was marginally faster than the mineral diesel-fuelled engine, indicating faster alkalinity loss in the KB20 fuelled engine. It appears that corrosion inhibitors (additives)

Table 6
Surface Roughness Profiles of Liner 1 from diesel and KB20 fuelled engines on the thrust (T) and anti-thrust (AT) sides.

	Diesel (Before the Endurance Test)	Diesel (After the Endurance Test)	KB20 (After the Endurance Test)
TDC, AT	 Ra=0.20, Rq=0.37	 Ra=0.21, Rq=0.40	 Ra=0.16, Rq=0.28
TDC, T	 Ra=0.22, Rq=0.41	 Ra=0.22, Rq=0.34	 Ra=0.22, Rq=0.29
MID, AT	 Ra=0.24, Rq=0.40	 Ra=0.09, Rq=0.20	 Ra=0.11, Rq=0.21
MID, T	 Ra=0.20, Rq=0.42	 Ra=0.13, Rq=0.25	 Ra=0.09, Rq=0.18
BDC, AT	 Ra=0.37, Rq=0.57	 Ra=0.32, Rq=0.46	 Ra=0.24, Rq=0.43
BDC, T	 Ra=0.28, Rq=0.49	 Ra=0.28, Rq=0.46	 Ra=0.27, Rq=0.45

deplete relatively faster in the KB20-fuelled engine due to their interaction with biodiesel entering the lubricating oil sump via fuel dilution/crankcase blow-by.

3.3.5. Flash point temperature

Lubricating oil molecules experience Van der Waals forces when heated. Fuel dilution of the lubricating oil is undesirable because it reduces the Van der Waals forces, lowering the flashpoint temperature [54]. The flashpoint temperatures of the lubricating oil samples drawn from mineral diesel and KB20 fuelled engines are shown in Fig. 10. For both test fuels, the flashpoint temperature of lubricating oil samples decreased with usage. Compared to the baseline mineral diesel-fuelled engine, a relatively lower reduction in the flashpoint temperature for KB20 fuelled engines was observed, suggesting the possibility of fuel dilution of the lubricating oil. Due to the lower flash point temperature of mineral diesel (49.5 °C) compared to Karanja biodiesel (168 °C), despite higher dilution, lower depression in the flash point temperature of lubricating oil from the KB20 fuelled engine is possible.

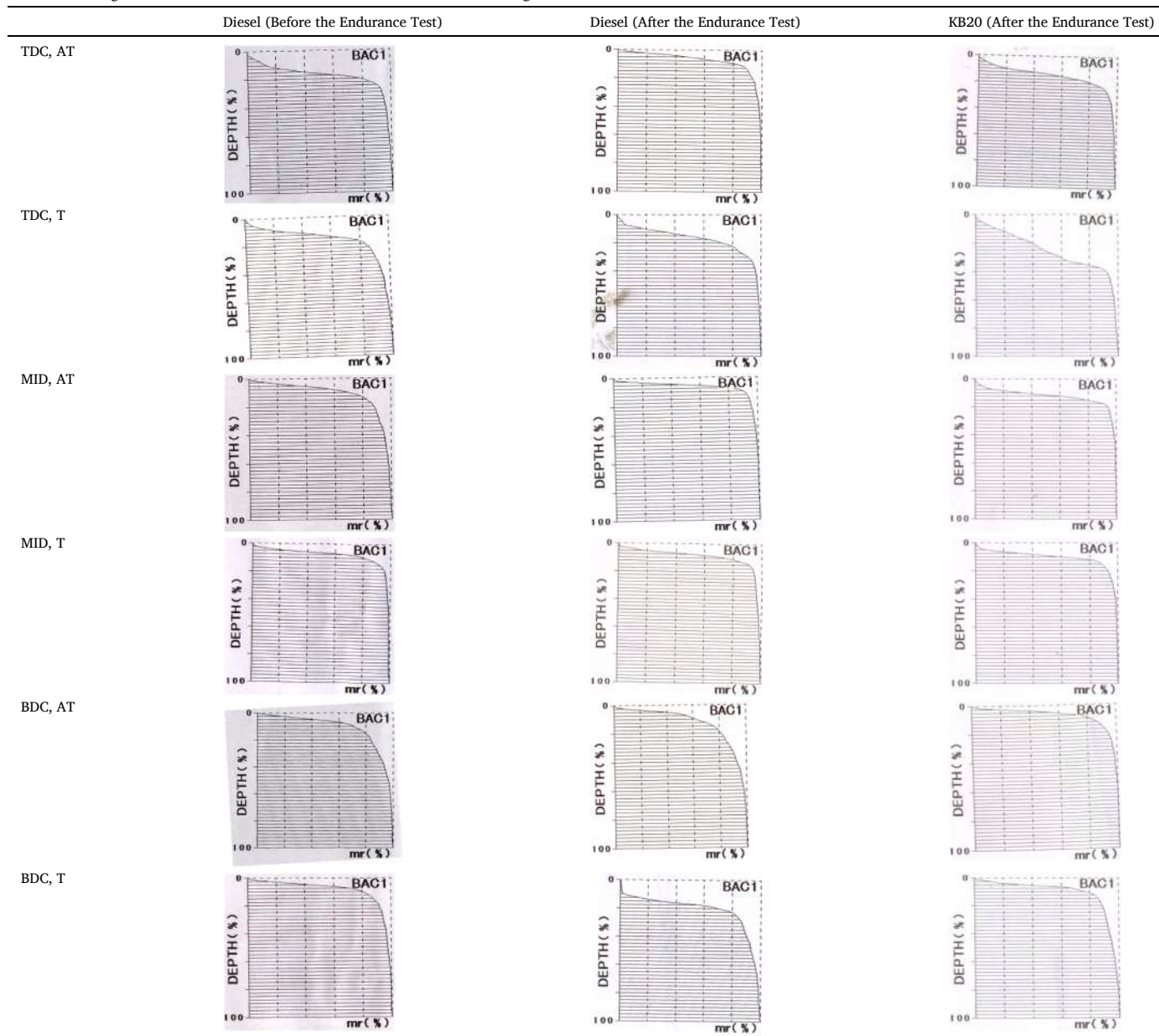
3.3.6. Moisture

Higher moisture content in the lubricating oil promotes oxidation of lubricating oil base stock, resulting in ‘additives drop-out,’ i.e., the precipitation of additives from the lubricant. Moisture traces aid rust formation and corrosion of various metallic surfaces, which enhance engine wear. Sources of moisture in the lubricating oil are typically blow-by gas, coolant leakage, etc. Lower engine blow-by occurs because of a properly sealed piston ring-liner interface, resulting in less moisture condensing in the lubricating oil in the engine crankcase. The moisture content differences in lubricating oil samples drawn from mineral diesel and KB20 fuelled engines were below 200 ppm, which was the lowest detection limit of the instrument used in these investigations. Hence no definite conclusions could be drawn from this test.

3.3.7. Copper corrosion

A copper corrosion bath and an ASTM standard plate for copper corrosion were used to verify the corrosiveness of lubricating oil to the copper-containing engine components. Fresh lubricating oil matched

Table 7
Surface Bearing Area Curves for Liner 1 from diesel and KB20 fuelled engine on the thrust and anti-thrust sides.



the grade '1a' in the ASTM standard plate, light orange and identical to a freshly polished copper strip. Even after 100 h of usage, the copper corrosiveness ratings of all lubricating oil samples from both engines were '1a.' As a result, it can be concluded that KB20 fuel did not cause any additional harm to the copper-containing components of the engine. Richard and McTavish [57] concluded that the inclusion of FAME (biodiesel) reduced the corrosion enactment of diesel engine oils, owing to double bonds in the FAME. The corrosion efficiency of lubricant samples was measured using the high-temperature corrosion bench test (HTCBT) (ASTM D6594), both with and without the inclusion of biodiesel in their investigations [57].

3.3.8. Pentane and toluene insoluble

Pentane and toluene are also organic solvents with different molecular structures; therefore, they have different preferential solubilities of different products. Pentane is an aliphatic hydrocarbon that only dissolves the lubricating oils, and the resinous compounds that may normally be soluble in the lubricating oil are discarded as insoluble in

pentane. Sludge produced during lubricating oil oxidation, metallic wear debris, carbonaceous soot, and foreign particles entering the environment constitute pentane insoluble. On the other hand, toluene is an aromatic organic solvent that can dissolve even the resinous materials produced in the lubricating oil by polymerization. Hence insoluble in toluene have a lower mass than the pentane insoluble. Hence the difference between the pentane and toluene insoluble indicates the extent of polymerization of the lubricating oil base-stock. ASTD D893 was used to determine the amount of pentane and toluene insoluble in the lubricating oil samples from mineral diesel and KB20 fuelled engines. The differences in pentane and toluene insoluble in the lubricating oil samples with usage are seen in Fig. 11.

Lubricating oil samples drawn from the KB20-fuelled engine exhibited higher levels of pentane insoluble. Since biodiesel has oxygen in its molecular structure, lubricating oil from biodiesel-fuelled engines is more susceptible to oxidation. It is reported in the literature that in the presence of sunlight and moisture, biodiesel is prone to oxidation [58–60], and this could also accelerate the oxidation of lubricating oil

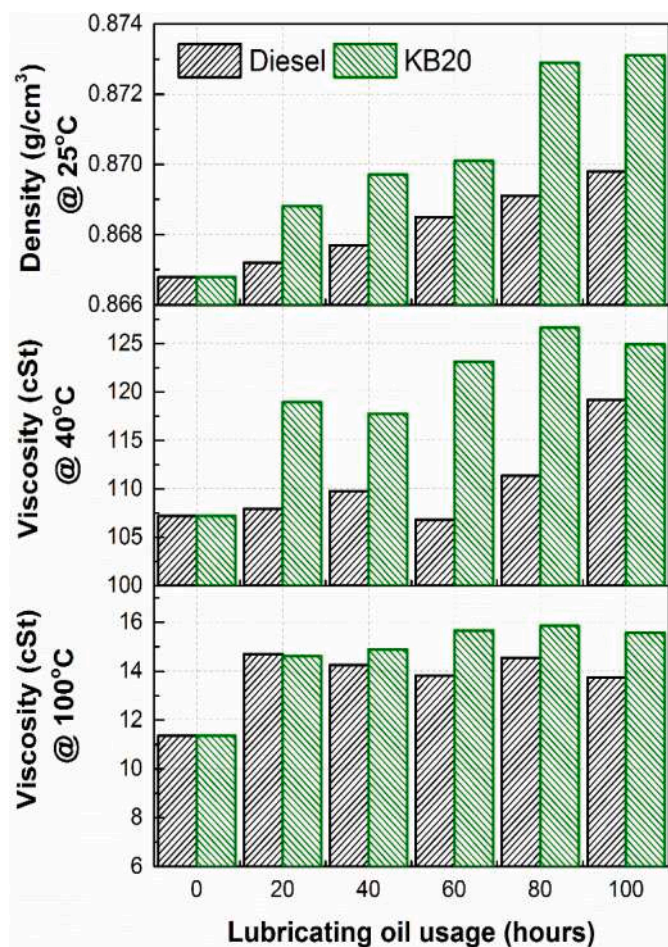


Fig. 9. (a) density at 25 °C, (b) viscosity at 40 °C, and (c) viscosity at 100 °C, of the lubricating oil samples drawn from KB20 and diesel-fuelled engines.

base-stock. According to Anwar and Garforth [61], oxidative stability is the time taken for fuel to be completely oxidized by atmospheric oxygen. Biodiesel oxidation produces undesirable by-products that threaten the engine components. The toluene insoluble of lubricating oil samples drawn from the KB20-fuelled engine was also higher than baseline mineral diesel-fuelled engine. Due to the induction of Karanja biodiesel in the lubricating oil via fuel dilution, oxidation of lubricating oil base-stock increased, forming a higher amount of resinous polymeric material in the lubricating oil samples from the KB20 fuelled engine.

3.3.9. Wear metals

Metallic wear debris generated due to component wear are washed away by the lubricating oil in any diesel engine. They eventually accumulate in the lubricating oil sump over a period of time. Information regarding component wear rate, the origin of trace metals, and engine condition can be predicted by evaluating trace metal concentration increase in the lubricating oil with usage. Inductively coupled plasma-optical emission spectroscopy (ICP-OES) was used to determine the wear trace metal concentration in the lubricating oil samples drawn from mineral diesel and KB20-fuelled engines.

Aluminum: The wear of pistons, bearings, dirt, additives, and thrust washers all contribute to aluminum in the lubricating oil. Except for a 20 h use sample from the diesel-fuelled engine, aluminum traces in the lubricating oil samples from KB20 and diesel-fuelled engines were <5 ppm (Fig. 12). However, compared to the baseline diesel-fuelled engine, the KB20-fuelled engine exhibited a slightly higher trace concentration of aluminum in the lubricating oil samples.

Magnesium: Magnesium in wear debris may originate from various

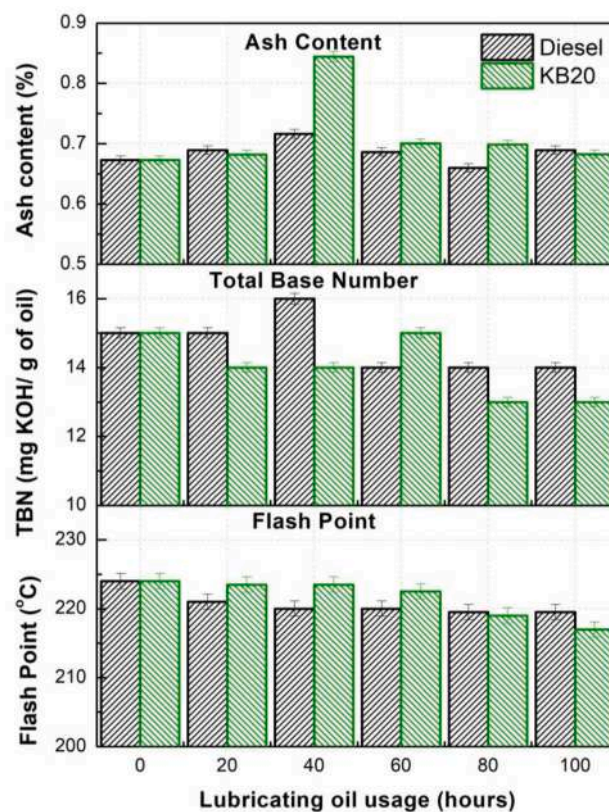


Fig. 10. Variations in (a) ash content, (b) total base number, and (c) flash point temperature of the lubricating oil samples drawn from KB20 and diesel-fuelled engines.

sources, including additive depletion, cylinder liner wear, bearing wear, etc. magnesium-containing compounds are used as the detergents (additives) in the lubricating oils. Magnesium concentration in the lubricating oil varied only marginally with both test fuels and remained at ~10 ppm (Fig. 12). For both phases, Magnesium trace concentration in the lubricating oil samples did not increase with usage.

Calcium: Calcium in the lubricating oil samples may have originated from additives, water, or grease. Calcium trace concentrations were slightly higher in the lubricating oil samples from the KB20-fuelled engine than mineral diesel-fuelled engine (Fig. 12). The calcium concentration in lubricating oil samples didn't increase significantly from the initial value in the fresh lubricating oil in both phases. This indicated that during usage, trace concentration addition in the lubricating oil was minimal.

Zinc: Zinc Di-alkyl Di-thio Phosphate (ZDDP), a zinc-containing compound, is a multi-functional additive used in lubricating oil formulations. ZDDP serves as an anti-oxidant, anti-wear, and extreme pressure additive as well as detergent. Organo-metallic complexes applied as additives in the lubricating oil produce zinc as trace metals. Zinc in the lubricating oil originates from additive depletion, bearing wear, brass parts, and neoprene seals, among other minor sources. Initial zinc concentration in the lubricating oil remained relatively constant over time in both phases of the engine endurance test. There was no significant effect of the use of KB20 on zinc trace concentrations in the lubricating oil samples drawn periodically (Fig. 12).

Chromium: Wear of cylinder liner, compression rings, crankshaft, and bearings could be the source of chromium in the lubricating oil. The chromium traces in the lubricating oil samples were very low, even after 40 h of engine operation. However, after 40 h, the KB20-fuelled engine showed increased chromium trace concentration in the lubricating oil (Fig. 12). The weight loss of piston rings was also measured, and the KB20 fuelled engine's piston rings clearly showed higher wear (Fig. 7).

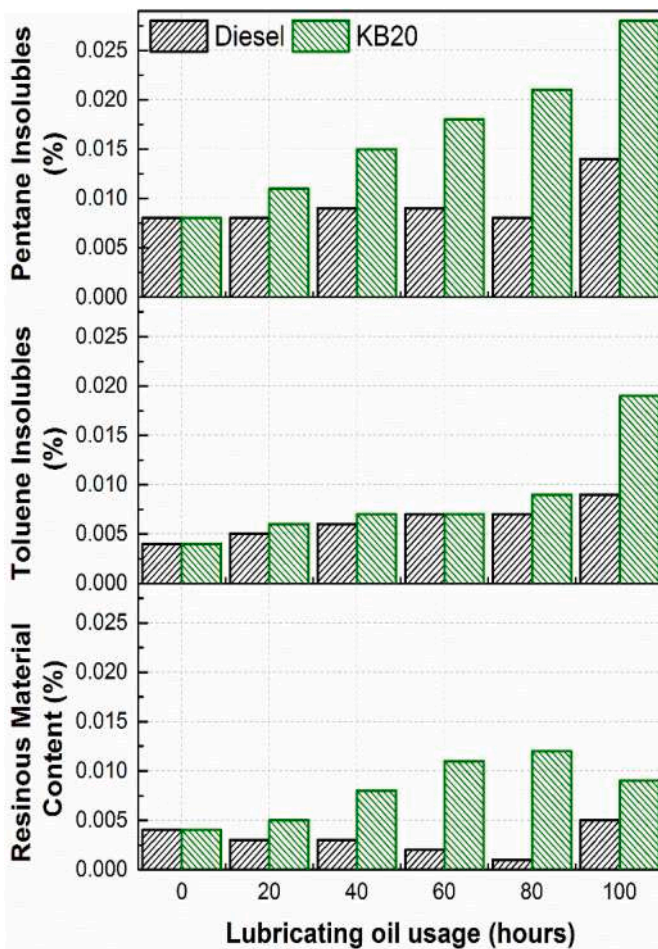


Fig. 11. Variations in (i) Pentane insoluble, (ii) Toluene insoluble, and (iii) Resinous material content of the lubricating oil samples drawn from KB20 and diesel-fuelled engines.

Friction between the piston ring and the liner is always susceptible to recurrent mechanical and thermal stresses at the contact interface, leading to fatigue-induced wear in the top layer of the ring. This may lead to surface damage because of the piston ring face coatings' pitting, spalling, and delamination [62,63]. Therefore, it is safe to assume that higher chromium trace concentrations in the lubricating oil samples drawn from KB20-fuelled engines were due to increased wear of piston rings.

Manganese: Wear of valves, steel shafts, etc., are sources of manganese in the lubricating oil with usage. Manganese was detected in very small trace concentration (<2 ppm) in the lubricating oil samples drawn from the engines using both the test fuels (Fig. 12), and its trace concentration did not change significantly over time.

Sodium: Coolant and additives are the two main sources of sodium in the lubricating oil. With usage, the sodium trace concentration in the lubricating oil drawn from mineral diesel and KB20 fuelled engines remained nearly constant (~2 ppm) and did not vary with time/usage (Fig. 12).

Copper: Wear of bearings, bushings, valve guides, and other components contribute to copper traces in the lubricating oil. With increased use, the trace concentrations of copper in the lubricating oil of both KB20 and diesel-fuelled engines increased significantly (Fig. 12). The increasing trace concentration of copper suggested the possibility of deteriorating lubrication effectiveness with usage due to lubricating oil oxidation. This would have resulted in increased wear of copper-containing components such as bearings over time.

Iron: Wear debris from cylinder liner, piston, rings, valves, shafts,

bearings, crankshaft, and corrosion are the main sources of iron in the lubricating oil. The wear of iron components in mineral diesel and KB20 fuelled engines was almost identical up to 40 h of engine operation in both phases (Fig. 12). The iron trace concentration in the lubricating oil samples drawn from the KB20 fuelled engine increased significantly and distinctly beyond this point, which exhibited a higher wear rate of iron components in the KB20 fuelled engine. This could be possibly due to higher oxidation and rusting of the engine components in the KB20 fuelled engine. Physical wear tests conducted in this study also corroborated these findings (Table 5).

Nickel: The primary sources of nickel in the lubricating oil are additives and wear debris from bearings, valves, and gear plating. The trace concentrations of nickel in the lubricating oils samples drawn from mineral diesel and KB20-fuelled engines was very low (<1 ppm), and they remained unchanged with usage.

Barium: Additives, water, and grease are the sources of Barium in the lubricating oil. The trace concentration of Barium in the lubricating oil samples drawn in both phases was very low (~0.1 ppm) and remained relatively stable with usage.

Lead: Wear of bearings, paints, and grease is the source of Lead in the lubricating oil. For both KB20 and mineral diesel-fuelled engines, Lead traces in the lubricating oil were less than 0.5 ppm and did not vary with usage.

Similarly, In the lubricating oil samples drawn from mineral diesel and KB20 fuelled engines, trace concentrations of potassium were ~1 ppm, while the trace concentrations of cobalt, copper, and beryllium were negligible. This section therefore does not include the curves showing variation of trace concentrations of these metals in the lubricating oil samples from both phases with usage.

3.4. Material compatibility

Various materials used in different engine components may be attacked by biodiesel, which is chemically more reactive than baseline mineral diesel. Therefore, before implementing biodiesel as an alternative fuel on a large scale, it is essential to determine the effect of Biodiesel/blends on the vital engine components. Table 8 shows the material compatibility observations of some of the critical engine components from this study.

The fuel system, especially the CRDI fuel pump and high-pressure solenoid injectors, was adversely affected by KB20. Relatively higher fuel viscosity of biodiesel caused the injectors to spray lesser fuel quantity with larger droplets into the engine combustion chamber than baseline mineral diesel. This led to a greater degree of incomplete combustion and higher smoke generation with KB20, resulting in higher carbonaceous deposits in the combustion chamber on the cylinder head, piston top, and injector tip. Gupta and Agarwal [64] performed macroscopic and microscopic spray characterization in the 500–1500 bar FIP range, using a solenoid injector for biodiesel blends (KB20 and KB40) and baseline mineral diesel. It emerged that the droplet size distribution represented by the Sauter mean diameter (SMD) (D_{32}) and arithmetic mean diameter (AMD) (D_{10}) increased with increasing biodiesel content in the test fuel. This was a piece of evidence that larger droplets constituted biodiesel blend sprays. This was because of the higher viscosity and surface tension of biodiesel than baseline mineral diesel. Relatively inferior low-temperature flow characteristics and higher unsaturation of biodiesel caused a higher degree of polymer formation in the test fuel, which clogged fuel filters frequently. Biodiesel and blends were accompanied by moisture, that was very difficult to remove and it caused severe damage to the fuel pump and injector, leading to internal corrosion. Seals and gaskets were also examined after the conclusion of both phases of the long-term endurance test. No significant damage was observed on the seals, and no difference in the wear pattern was observed during both these phases.

According to this table, the use of biodiesel in modern CRDI engines can increase the maintenance costs. This observation was in stark

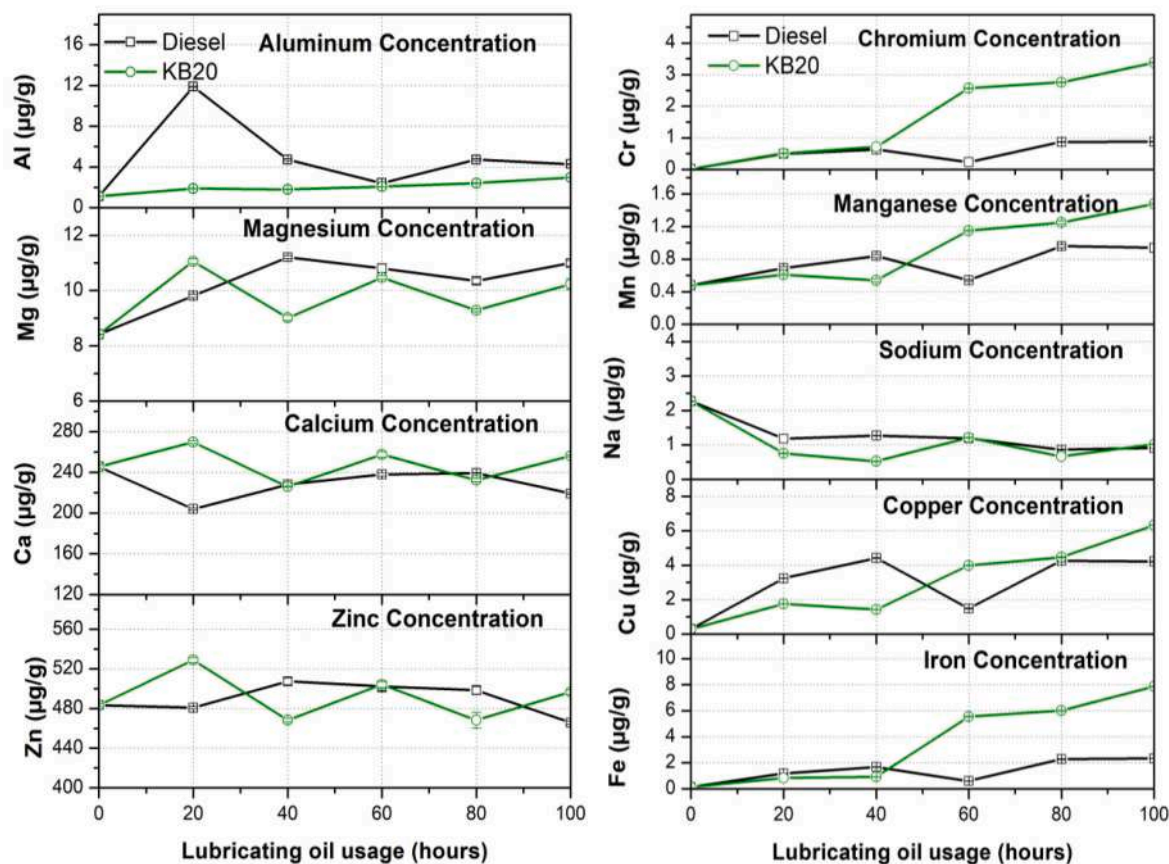


Fig. 12. Variations in the trace concentrations of (a) Aluminum, (b) Magnesium, (c) Calcium, (d) Zinc, (e) Chromium, (f) Manganese, (g) Sodium, (h) Copper and (i) Iron in the lubricating oil samples drawn from KB20 and diesel-fuelled engines.

Table 8
Material compatibility of engine components with KB20 vis-a-vis baseline mineral diesel.

Component	Relative condition for KB20 compared to baseline mineral diesel
Valves	Wear of inlet and outlet valves was lower by ~30–50% in KB20.
Liner	Direct comparison was not meaningful because the liner was integral to the block and was not changed in the two phases. Higher wear was noticed for KB20 from the surface profiles that are given separately.
Piston	Wear was slightly higher in KB20.
Piston rings	200–300% higher wear in KB20. Highest wear in top compression ring for KB20.
Gudgeon pin	20–30% higher wear in KB20.
Small/big end bearing of connecting rod	20–30% higher wear in KB20.
Crankpin	10–20% lower wear in KB20.
Main bearing	40–50% higher wear in KB20.
Lubricating oil	Tribological investigation data is provided separately.
Carbon deposits on Piston, Cylinder head, and Injectors	Photographs of each are given separately. Higher deposits on KB20 engine components.
Head gasket	No difference.
Intake manifold gasket	No difference.
Exhaust manifold gasket	No difference.
Rubber Components	No rubber components in the engine.
Timing belt	Severe damage in the KB20 engine.
Turbocharger	No difference.
Fuel injectors	Damaged during second phase endurance test on KB20 after 132 h and were replaced.

contrast to the observations made by several other scientific studies, which showed an exactly opposite trends while using relatively older (Euro-3/2/1/0) engines. The differences observed were due to specific engine design features, especially the fuel injection equipment, which employed very high fuel injection pressures of ~1400–1600 bar. Therefore, it is recommended that the OEMs check biodiesel compatibility of an engine before it is allowed to operate on biodiesel for extended periods, and a suitable warranty and maintenance protocol is then offered to the end-user.

4. Conclusions

An endurance test on a CRDI diesel engine typically used in SUVs was performed to compare the effects of KB20 w.r.t. baseline mineral diesel. Engine wear of important engine components before and after the 274-h endurance test on each fuel was assessed. Carbon deposits on the engine components such as the cylinder head, piston top, and fuel injectors were considerably higher in case of KB20. Physical dimensions of engine components were measured before and after the endurance test in both phases, which indicated substantially lower wear on the valves and crankpins of the KB20-fuelled engine. The KB20-fuelled engine, on the other hand, displayed higher wear of the liners, piston rings, pistons, gudgeon pin, small and big end bearings of the connecting rod, and the main bearings. Various oil tribology tests performed on the lubricating oil samples from mineral diesel and KB20 fuelled engines exhibited the influence of fuel chemistry on the lubricating oil efficacy and its residual useful life. Lubricating oil from the KB20-fuelled engine exhibited a higher increase in density and ash content. The viscosity tests indicated that the lubricating oil drawn from the KB20 fuelled engine underwent higher oxidation and polymerization. Greater resinous content in the

lubricating oil from the KB20-fuelled engine also indicated higher lubricating oil oxidation and polymerization. With use, wear debris accumulated in the lubricating oil, increasing the trace metal concentration. The lubricating oil samples drawn from the KB20 fuelled engine exhibited higher traces of Cr and Fe. However, Al, Mg, Ca, Zn, Mn, and Na trace concentrations were almost identical in all lubricating oil samples and didn't change significantly with usage. The biodiesel blends harmed the CRDI engine's fuel injection system though. If enough additives are added to biodiesel, this negative influence on the fuel injection system can be eliminated. This study concludes that Karanja biodiesel blends may be utilized as a partial substitute for mineral diesel (up to 20%), with modest recalibration of the ECU, with minor changes in the lubricating oil composition, and without any substantial changes in the engine hardware.

CRedit authorship contribution statement

Jai Gopal Gupta: Data curation, Formal analysis, Investigation, Writing – original draft. **Avinash Kumar Agarwal:** Conceptualization, Methodology, Project administration, Resources, Supervision, Writing – review & editing.

Declaration of competing interest

The authors declare that they have no known competing financial interests or personal relationships that could have appeared to influence the work reported in this paper.

Acknowledgments

Research funding by the Technology Systems Group of the Department of Science and Technology, Government of India, is gratefully acknowledged, which enabled us to undertake this project (Grant No. DST/TSG/AF/2007/20 dated February 4, 2010). The authors acknowledge the assistance of Sh. Veeramani and Tata Motors, Pune for providing the test engine and other required hardware for experiments of this study to the Engine Research Laboratory, Indian Institute of Technology Kanpur, India.

References

- [1] H. Yaqoob, Y.H. Teoh, F. Sher, M.A. Jamil, D. Murtaza, M. Al Qubeissi, M. U Hassan, M.A. Mujtaba, Current status and potential of tire pyrolysis oil production as an alternative fuel in developing countries, *Sustainability* 13 (6) (2021 Jan) 3214.
- [2] K.N. Gopal, R.T. Raj, Effect of Pongamia oil methyl ester–diesel blend on lubricating oil degradation of DI compression ignition engine, *Fuel* 165 (2016) 105–114.
- [3] A. Dhar, A.K. Agarwal, Effect of Karanja biodiesel blend on engine wear in a diesel engine, *Fuel* 134 (2014) 81–89.
- [4] D. Tziourtzioumis, A. Stamatelos, Effects of a 70% biodiesel blend on the fuel injection system operation during steady-state and transient performance of a common rail diesel engine, *Energy Convers. Manag.* 60 (2012) 56–67.
- [5] M.A. Fazal, A.S.M.A. Haseeb, H.H. Masjuki, Biodiesel feasibility study: an evaluation of material compatibility; performance; emission, and engine durability, *Renew. Sustain. Energy Rev.* 15 (2011) 1314–1324.
- [6] O. Armas, S. Martínez-Martínez, C. Mata, Effect of an ethanol–biodiesel–diesel blend on a common rail injection system, *Fuel Process. Technol.* 92 (11) (2011) 2145–2153.
- [7] S. Peñan, M.S. Jerman, M. Kegl, B. Kegl, Biodiesel influence on tribology characteristics of a diesel engine, *Fuel* 88 (6) (2009) 970–979.
- [8] A.K. Agarwal, J. Bijwe, L.M. Das, Effect of biodiesel utilization on the wear of vital parts in compression ignition engine, *ASME. J. Engg. Gas Turb. Power* 125 (2003) 604–611.
- [9] Staat F, Gateau P. The Effects of Rapeseed Oil Methyl Ester on Diesel Engine Performance, Exhaust Emissions and Long-Term Behavior - a Summary of Three Years of Experimentation. SAE Paper No. 950053.
- [10] Sem TR. Effect of various lubricating oils on piston deposits in biodiesel fuelled engines. SAE Paper No. 2004-01-0098.
- [11] M.A. Fazal, A.S.M.A. Haseeb, H.H. Masjuki, Comparative corrosive characteristics of petroleum diesel and palm biodiesel for automotive materials, *Fuel Process. Technol.* 91 (2010) 1308–1315.
- [12] S. Kaul, R.C. Saxena, A. Kumar, M.S. Negi, A.K. Bhatnagar, H.B. Goyal, A.K. Gupta, Corrosion behavior of biodiesel from seed oils of Indian origin on diesel engine parts, *Fuel Process. Technol.* 88 (2007) 303–307.
- [13] Besee GB, Fay JP. Compatibility of Elastomers and Metals in Biodiesel Fuel Blends. SAE Paper No. 971690.
- [14] Gerpen JV. Determining the Influence of Contaminants on Biodiesel Properties. SAE Paper No. 971685.
- [15] Schumacher L., Borgelt S.C., Hires W.G., Wetherell W., Nevils A., 100,000 Miles of Fueling 5.9l Cummins Engines with 100% Biodiesel. SAE Paper No. 962233.
- [16] A.K. Agarwal, S. Park, A. Dhar, C.S. Lee, S. Park, T. Gupta, N.K. Gupta, Review of experimental and computational studies on spray, combustion, performance, and emission characteristics of biodiesel fuelled engines, *ASME. J. Energy Resour. Technol.* 140 (12) (2018) 1–30, 120801.
- [17] A.T. Hoang, M. Tabatabaei, M. Aghbashlo, A.P. Carlucci, A.I. Ölçer, A.T. Le, A. Ghassemi, Rice bran oil-based biodiesel as a promising renewable fuel alternative to petrodiesel: a review, *Renew. Sustain. Energy Rev.* 135 (2020) 112024.
- [18] F.J. Owuna, Stability of vegetable-based oils used in the formulation of eco-friendly lubricants—a review, *Egyptian Journal of Petroleum* 29 (3) (2020) 251–256.
- [19] Y.C. Lin, W.J. Lee, T.S. Wu, C.T. Wang, Comparison of PAH and regulated harmful matter emissions from biodiesel blends and paraffinic fuel blends on engine accumulated mileage test, *Fuel* 85 (2006) 2516–2523.
- [20] A.K. Agarwal, D. Agarwal, Field-testing of biodiesel (B100) and diesel-fueled vehicles: Part 3—wear assessment of liner and piston rings, engine deposits, and operational issues, *J. Energy Resour. Technol.* 143 (4) (2021 April 1), 042309.
- [21] A.K. Agarwal, D. Agarwal, Field-testing of biodiesel (B100) and diesel-fueled vehicles: Part 4—piston rating, and fuel injection equipment issues, *J. Energy Resour. Technol.* 143 (4) (2021 April 1), 042310.
- [22] A. Dhar, A.K. Agarwal, Experimental investigations of the effect of Karanja biodiesel on tribological properties of lubricating oil in a compression ignition engine, *Fuel* 130 (2014) 112–119.
- [23] M.S. Dandu, K. Nanthagopal, Clean Karanja methyl ester compatibility study on long term tribological behavior of a compression ignition engine, *Fuel* 291 (2021) 120148.
- [24] M. Thornton, T. Alleman, J. Luecke, R. McCormick, Impacts of biodiesel fuel blends oil dilution on light-duty diesel engine operation, *SAE International Journal of Fuels and Lubricants* 2 (1) (2009) 781–788.
- [25] A.K. Agarwal, J. Bijwe, L.M. Das, Wear assessment in a biodiesel fuelled compression ignition engine, *ASME. J. Engg. Gas Turb. Power* 125 (2003) 820–826.
- [26] J. Sentanuhady, W. Saputro, M.A. Muflikhun, Metals and chemical compounds contaminants in diesel engine lubricant with B20 and B100 biofuels for long-term operation, *Sustainable Energy Technologies and Assessments* 45 (2021 June 1) 101161.
- [27] Reece DL, Peterson CL. Biodiesel Testing in Two On-Road Pickups. SAE Paper No. 952757.
- [28] M.H. Mosarof, M.A. Kalam, H.H. Masjuki, A. Alabdulkarem, A.M. Ashraf, A. Arslan, H.K. Rashedul, I.M. Monirul, Optimization of performance, emission, friction, and wear characteristics of palm and Calophylluminophyllum biodiesel blends, *Energy Convers. Manag.* 118 (2016) 119–134.
- [29] A. Murugesan, C. Umarani, R. Subramanian, N. Nedunchezian, Bio-diesel as an alternative fuel for diesel engines—a review, *Renew. Sustain. Energy Rev.* 13 (3) (2009 April 1) 653–662.
- [30] C. Patel, K. Chandra, J. Hwang, R.A. Agarwal, N. Gupta, C. Bae, T. Gupta, A. K. Agarwal, Comparative compression ignition engine performance, combustion and emission characteristics, and trace metals in particulates from Waste cooking oil, Jatropa, and Karanja oil derived biodiesels, *Fuel* 236 (2019) 1366–1376.
- [31] S. Raadnu, A. Meenak, Effects of refined palm oil (RPO) fuel on wear of diesel engine components, *Wear* 254 (2003) 1281–1288.
- [32] L. Schumacher, J.V. Gerpen, Engine Oil Analysis of Diesel Engines Fuelled with 0, 1, 2, and 100 Percent Biodiesel. ASAE Annual Meeting, Midwest Express Center Milwaukee, WI, 9-12 July 2000. Paper No. 00-6010.
- [33] G.K. Mistri, S.K. Aggarwal, D. Longman, A.K. Agarwal, Performance and emission investigations of Jatropa and Karanja biodiesels in a single-cylinder compression-ignition engine using endoscopic imaging. *ASME. J. Energy Resour. Technol.* 138 (1) (2016) 1–13, 011202.
- [34] Indian Standard IS: 10000, Method of Tests for Internal Combustion Engine: Part IX, Endurance Tests, 1980, Bureau of Indian Standards, New Delhi, India.
- [35] Indian Standard IS: 10000, Method of Tests for Internal Combustion Engine: Part V, Preparation for Tests and Measurements for Wear, Bureau of Indian Standards, New Delhi, India, 1980.
- [36] M. García-Morales, S.D. Fernández-Silva, C. Roman, M.A. Delgado, Electro-active control of the viscous flow and tribological performance of ecolubricants based on phyllosilicate clay minerals and castor oil, *Appl. Clay Sci.* 198 (2020 Nov 15) 105830.
- [37] H. Yaqoob, Y.H. Teoh, F. Sher, M.U. Ashraf, S. Amjad, M.A. Jamil, M.M. Jamil, M. A. Mujtaba, Jatropa curcas biodiesel: a lucrative recipe for Pakistan's energy sector, *Processes* 9 (2021) 1129.
- [38] H. Yaqoob, Y.H. Teoh, F. Sher, M.A. Jamil, M. Nuhanović, O. Razmkhah, B. Erten, Tribological behaviour and lubricating mechanism of tire pyrolysis, oil. *Coatings* 11 (4) (2021 Apr) 386.
- [39] H. Yaqoob, Y.H. Teoh, M.A. Jamil, T. Rasheed, F. Sher, An experimental investigation on tribological behaviour of tire-derived pyrolysis oil blended with biodiesel fuel, *Sustainability* 12 (23) (2020 Jan) 9975.

- [40] Y.H. Teoh, H.G. How, F. Sher, T.D. Le, H.T. Nguyen, H. Yaqoob, Fuel injection responses and particulate emissions of a CRDI engine fueled with *cocos nucifera* biodiesel, *Sustainability* 13 (9) (2021 Jan) 4930.
- [41] M. Habibullah, H.H. Masjuki, M.A. Kalam, N.W. Zulkifli, B.M. Masum, A. Arslan, M. Gulzar, Friction and wear characteristics of *Calophyllum inophyllum* biodiesel, *Ind. Crop. Prod.* 76 (2015) 188–197.
- [42] A.K. Agarwal, A. Dhar, Effect of Karanja biodiesel blend on engine wear in a diesel engine, *Fuel* 134 (2014) 81–89.
- [43] J.G. Gupta, A.K. Agarwal, S.K. Aggarwal, Particulate emissions from Karanja biodiesel fuelled turbocharged CRDI sports utility vehicle engine, *ASME. J. Energy Resour. Technol.* 137 (6) (2015) 1–6, 064503.
- [44] Fraer R, Dinh H, Proc K, McCormick RL, Chandler K, Buchholz B. Operating Experience and Teardown Analysis for Engines Operated on Biodiesel Blends (B20). SAE Paper No. 2005-01-3641.
- [45] Birgel A, Ladommatos N, Aleiferis P, Zuelch S, Milovanovic N, Lafon V, Orlovic A, Lacey P, Richards P. Deposit Formation in the Holes of Diesel Injector Nozzles: a Critical Review. SAE Paper No. 2008-01-2383.
- [46] Verhaeven E, Pelkmans L, Govaerts L, Lamers R, Theunissen F. Results of Demonstration and Evaluation Projects of Biodiesel from Rapeseed and Used Frying Oil on Light and Heavy-Duty Vehicles. SAE Paper No. 2005-01-2201.
- [47] S. Sinha, A.K. Agarwal, Experimental investigation of the effect of biodiesel utilization on lubricating oil degradation and wear of a transportation CIDI engine, *ASME. J. Engg. Gas Turb. Power* 132 (2010) 1–9, 042801.
- [48] S.M. Reddy, N. Sharma, N. Gupta, A.K. Agarwal, Effect of non-edible oil and its biodiesel on wear of fuel injection equipment components of a genset engine, *Fuel* 222 (2018) 841–851.
- [49] Morcos M, Parsons G, Lauterwasser F, Boons M, Hartgers W. Detection Methods for Accurate Measurements of the FAME Biodiesel Content in Used Crankcase Engine Oil. SAE Paper No. 2009-01-2661.
- [50] W.P. Dong, E.J. Davis, D.L. Butler, K.J. Stout, Topographic features of cylinder liners—an application of three-dimensional characterization techniques, *Tribol. Int.* 28 (7) (1995 Nov 1) 453–463.
- [51] D.K. Srivastava, A.K. Agarwal, J. Kumar, Effect of liner surface properties on wear and friction in a non-firing engine simulator, *Mater. Des.* 28 (2007) 1632–1640.
- [52] R. Kumar, S. Kumar, B. Prakash, A. Sethuramiah, Assessment of engine liner wear from bearing area curves, *Wear* 239 (2000) 282–286.
- [53] C. Patel, J. Hwang, K. Chandra, R.A. Agarwal, C. Bae, T. Gupta, A.K. Agarwal, In-cylinder spray and combustion investigations in a heavy-duty optical engine fuelled with waste cooking oil, *Jatropha*, and *Karanja* biodiesels, *ASME. J. Energy Resour. Technol.* 141 (1) (2019) 1–12, 012201.
- [54] A.K. Agarwal, Experimental investigations of the effect of biodiesel utilization on lubricating oil tribology in diesel engines, *Journal of Auto. Engg., Proceedings of IMechE, Part-D* 219 (5) (2005) 703–714.
- [55] Smith LA, Preston WH, Dowd G, Taylor O, Wilkinson KM. Application of a First Law Heat Balance Method to a Turbocharged Automotive Diesel Engine. SAE Paper No. 2009-01-2744.
- [56] A.K. Agarwal, J.G. Gupta, R.K. Maurya, W.I. Kim, S. Lee, C.S. Lee, S. Park, Spray evolution, engine performance, emissions and combustion characterization of Karanja biodiesel fuelled common rail turbocharged direct injection transportation engine, *Int. J. Eng. Res.* 17 (10) (2016) 1092–1107.
- [57] K.M. Richard, S. McTavish, Impact of biodiesel on lubricant corrosion performance, *SAE International Journal of Fuels and Lubricants* 2 (2) (2010 January 1) 66–71.
- [58] R.K. Saluja, K. Vineet, S. Radhey, Stability of biodiesel – a review, *Renew. Sustain. Energy Rev.* 62 (2016) 866–881.
- [59] C. Sasikumar, K. Balamurugan, S. Jegadheeswaran, R. Sathyamurthy, Optimization of process parameter in the production of *Jatropha Methyl Ester* using response surface methodology, *Biocatalysis and Agricultural Biotechnology* 27 (2020) 101693.
- [60] C.B. Sia, J. Kandedo, Y.H. Tan, K.T. Lee, Evaluation on biodiesel cold flow properties, oxidative stability, and enhancement strategies: a review, *Biocatalysis and Agricultural Biotechnology* 24 (2020) 101514.
- [61] A. Anwar, A. Garforth, Challenges and opportunities of enhancing cold flow properties of biodiesel via heterogeneous catalysis, *Fuel* 173 (2016) 189–208.
- [62] S. Wan, H. Wang, Y. Xia, A.K. Tieu, B.H. Tran, H. Zhu, Investigating the corrosion-fatigue wear on CrN coated piston rings from laboratory wear tests and field trial studies, *Wear* 432 (2019 Aug 15) 202940.
- [63] A. Amanov, R. Karimbaev, S.P. Berkebile, Effect of ultrasonic nanocrystal surface modification on wear mechanisms of thermally-sprayed WC-Co coating, *Wear* (2021 Mar 20) 203873.
- [64] Gupta JG, Agarwal AK. Macroscopic and microscopic spray characteristics of diesel and Karanja biodiesel blends. SAE Paper No. 2016-01-0869.